Proceedings of the ASME 2018 Conference on Smart Materials, Adaptive Structures and Intelligent Systems
SMASIS2018
September 10-12, 2018, San Antonio, TX, USA

SMASIS2018-8153

ELECTRO-ACTIVE POLYMER BASED SELF-FOLDING APPROACH DEVOTED TO ORIGAMI-INSPIRED STRUCTURES

Amine Benouhiba*
Kanty Rabenorosoa
Patrick Rougeot
Morvan Ouisse
Nicolas Andreff
FEMTO-ST Institute
University of Bourgogne Franche-Comté/CNRS
25000 Besançon, France
Email: amine.benouhiba@femto-st.fr

ABSTRACT

In the growing field of origami engineering, self-folding is of a high regard. The latter is regularly used by nature as an efficient approach for autonomous growing and reorganizing. In this work, we present a self-folding approach based on Electro-Active Polymer (EAP), especially Conductive Polymers (CP). This approach proposes lightweight, compact and energy efficient self-folding structures, as well as large angle and reversible folding. We study the behavior of a three-segment milli-structure containing two passive segments made of paper, separated by an active segment made of CP. The folding motion of the structure was modeled and experimentally validated. Furthermore, as a proof of concept, a self-folding origami cube is presented.

Keywords: self-folding, electro-active polymer, active structures, origami-based structure.

NOMENCLATURE

m	Number of segments in the self-folding structure.
i	Index of the segment.
SF	Matrix of the self-folding structure.
C_P	Matrix used to express a passive segment.
l	Length of a passive segment.
C_A	Matrix used to express an active segment.
n	Number of points used to define the active segment.
j	Index of the points of the CP actuator curvature.
x_n	Coordinate of the tip of the active segment along the X-axis.
y_n	Coordinate of the tip of the active segment along the Y-axis.
z_n	Coordinate of the tip of the active segment along the Z-axis.
M	Homogeneous transformation matrix.
θ	Rotation around Z-axis (folding angle).
ϕ	Rotation around Y-axis (the segment's orientation angle).

1 Introduction

Origami is ancient Japanese art of paper folding, which date back to the 1600s. The fact that origami-based structures has the ability to be folded compactly into very small devices, which can be deployed at a later time into a larger state, makes it of an interest to the scientific and engineering communities. Various recent examples of origami-based devices include a space solar array [1], medical devices [2–5] or vibro-acoustic devices [6]. Of a special interest in the rapidly growing field of origami engineering is autonomous folding, also known as self-folding [7, 8]. Compared to the traditional engineering devices, actuating

*Address all correspondence to this author.

origami-based structures can be a bit of a challenge. Key parameters of such structures are the folding angles and their orientation (mount or valley), which make up the geometry of the desired state (shape and size). Usually, these angles are very wide, in order to achieve large volume and size variation. Furthermore, the actuation mechanism should be able to generate such wide angles while at the same time, keeping a small enough size to allow their integration into the systems and also to avoid self-collision. Different actuation methods designated to origami-based structures and self-folding systems have been proposed, such as EAP, especially Dielectric Elastomers (DE) [9], Shape Memory Alloys (SMA) [7, 10–12] and Shape Memory Polymers (SMP), which are found in heat-trigged systems [8, 13–16] and light-trigged systems [17–19].

In this paper we propose to use an EAP, especially, CP-based self-folding approach, devoted to milli-origami-inspired structures. This approach offers many advantages: beside its ability to produce very large angles while keeping a small size for simpler integration, it can be applied to origami-inspired structures. It is also, lightweight, energy efficient, low voltage activated and reversible. The approach is based on tri-layer CP actuators, whose certain regions were rigidified using structural layers (such as, paper or copper tape), while the remaining ones are kept free to enables the folding/unfolding of the structure. Choosing the regions depends on the design and the desired origami structure.

First, in section 2, a kinematic model for the CP-based self-folding approach, which is able to predict the folding/unfolding state of the structure, is proposed. Then, in section 3, the approach is experimentally validated and a proof of concept is presented. Finally, in section 4 concludes the paper and the applications as well as future work are discussed.

2 Model of the self-folding structure

This section introduces the model used for the description the kinematics a self-folding multi-segment CP actuators based structure. The latter is composed of passive segments (C_P^i) and active segments (C_A^i). Both kinds of segments can be represented in geometrical space (global frame R_0 as shown in Fig. 1)) on their own frames by the following matrices, respectively :

$$C_P^i = \begin{bmatrix} 0 & x_i \\ 0 & y_i \\ 0 & z_i \\ 1 & 1 \end{bmatrix}, \tag{1}$$

$$C_A^i = \begin{bmatrix} 0 & x_{i,1} & \dots & x_{i,n} \\ 0 & y_{i,1} & \dots & y_{i,n} \\ 0 & z_{i,1} & \dots & z_{i,n} \\ 1 & 1 & \dots & 1 \end{bmatrix}, \tag{2}$$

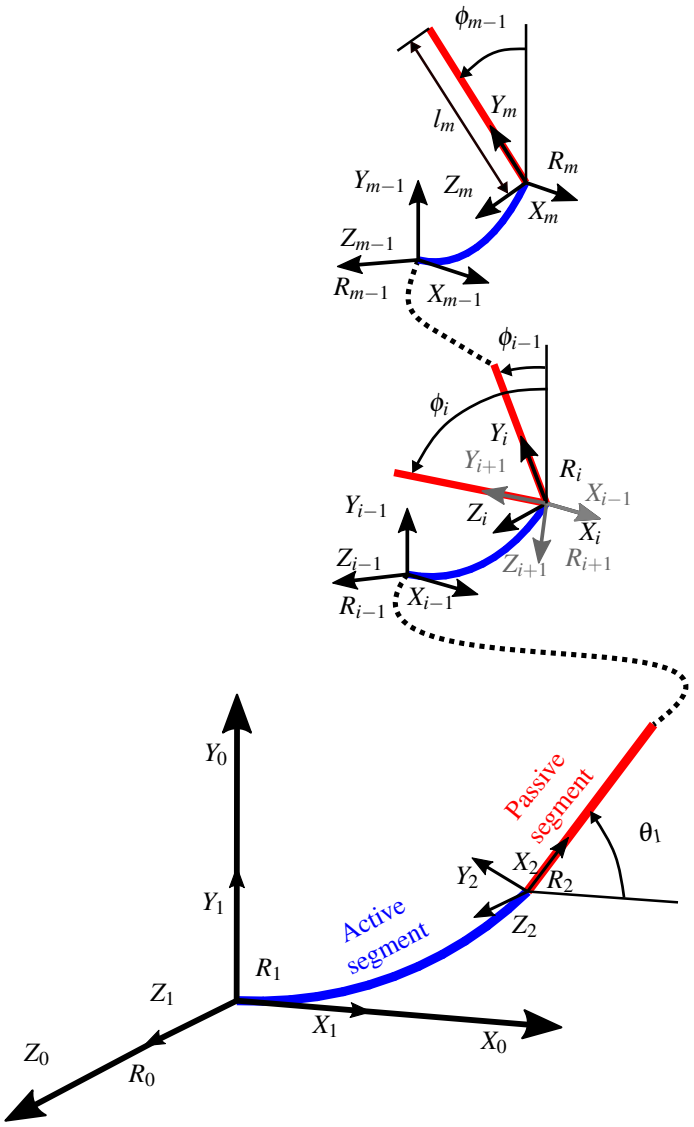

FIGURE 1. Coordinate system for the self-folding multi-segment structure.

Where x_i, y_i and z_i are the coordinates of the passive segment i, and $x_{i,j}$, $y_{i,j}$ and $z_{i,j}$ are the coordinates of the point j from the curvature of the active segment i. The curvature obtained the CP actuator is discretized into n points. They were determined using a multi-physics model. The latter takes the applied voltage as an input and gives the curvature of the CP actuator as an output. The multi-physics model is based on the work of Kim et *al.* [21] in order to take into account the large displacement of multilayer cantilevers. It is derived from the nonlinear Euler-Bernoulli beam equation and it utilizes three layers: two active layers separated by a passive layer. A few assumptions were considered in tri-layer CP actuator model:

– The material of each layer remains linearly elastic.
– Two consecutive layers are perfectly bonded.
– The radius of the curvature of the multilayer cantilever caused by combined effect of all stresses is much bigger than its thickness.

However, since the model of the curvature of the CP actuators goes behind the scope of this paper and for the sake of presentation, it will not be discussed here.
In order to find the coordinates of the full self-folding multi-segment structure with m segments, a transformation matrix is needed. Two kind of transformation matrices are defined depending on the nature of the segment. First when the $i-1$ segment is a passive one, the transformation matrix writes:

$$ {}^{i}M_{i-1} = \begin{bmatrix} \cos\phi_i\cos\theta_i & -\cos\phi_i\sin\theta_i & \sin\phi_i & x_{i-1} \\ \sin\theta_i & \cos\theta_i & 0 & y_{i-1} \\ -\sin\phi_i\cos\theta_i & \sin\phi_i\sin\theta_i & \cos\phi_i & z_{i-1} \\ 0 & 0 & 0 & 1 \end{bmatrix}, \quad (3) $$

Where θ_i is the rotation around Z-axis and ϕ_i is the rotation around Y-axis, of the segment i. Secondly, when the segment $i-1$ is an active segment, one has:

$$ {}^{i}M_{i-1} = \begin{bmatrix} \cos\phi_i\cos\theta_i & -\cos\phi_i\sin\theta_i & \sin\phi_i & x_{i-1,n} \\ \sin\theta_i & \cos\theta_i & 0 & y_{i-1,n} \\ -\sin\phi_i\cos\theta_i & \sin\phi_i\sin\theta_i & \cos\phi_i & z_{i-1,n} \\ 0 & 0 & 0 & 1 \end{bmatrix}, \quad (4) $$

Expressions (3) and (4) allow the representation of segment i in the frame of segment $i-1$, therefore, in order to express the i segment in the global frame (the frame of the first segment), the following equation is required:

$$ {}^{i}M_0 = \prod_{j=1}^{i} {}^{j}M_{j-1}. \quad (5) $$

Finally, using expressions (1), (2) and (5), the full self-folding structure can be expressed in the global frame by the concatenation of all the expressions of the m segments, as such:

$$ SF_m = \left[|{}^{1}M_0\, C_{P,A}^{1}| \;\; \ldots \;\; |\prod_{j=1}^{i} {}^{j}M_{j-1}\, C_{P,A}^{i}| \;\; \ldots \;\; |\prod_{j=1}^{m} {}^{j}M_{j-1}\, C_{P,A}^{m}| \right]. \quad (6) $$

2.1 Three-segment structure

In this subsection, a three-segment straight structure is modeled. The structure contains one active segment (CP actuator), linking two rigid segments moving in the (X_0,Y_0) plan. All the z coordinates as well as the rotation angle ϕ are null. The three segments are defined in their own frames R_1, R_2 and R_3, respectively, by the following matrices, for the first segment:

$$ C_P^1 = \begin{bmatrix} 0 & l_1 \\ 0 & 0 \\ 0 & 0 \\ 1 & 1 \end{bmatrix}, \quad (7) $$

for the second segment:

$$ C_A^2 = \begin{bmatrix} 0 & x_{2,1} & \ldots & x_{2,n} \\ 0 & y_{2,1} & \ldots & y_{2,n} \\ 0 & 0 & \ldots & 0 \\ 1 & 1 & \ldots & 1 \end{bmatrix}, \quad (8) $$

The coordinates of the curvature of the active segment, in expression (8), were determined using a electro-chemico-mechanical model as discussed above. Finally, the third segment:

$$ C_P^3 = \begin{bmatrix} 0 & l_3 \\ 0 & 0 \\ 0 & 0 \\ 1 & 1 \end{bmatrix}. \quad (9) $$

Then, in order to express the three segments in the global frame R_0 using the method discussed above, The following transformation matrices are required:

$$ {}^{1}M_0 = \begin{bmatrix} 1&0&0&0 \\ 0&1&0&0 \\ 0&0&1&0 \\ 0&0&0&1 \end{bmatrix}, {}^{2}M_1 = \begin{bmatrix} 1&0&0&l_1 \\ 0&1&0&0 \\ 0&0&1&0 \\ 0&0&0&1 \end{bmatrix}, \quad {}^{3}M_2 = \begin{bmatrix} cos\theta_3 & -sin\theta_3 & 0 & x_{2,n} \\ sin\theta_3 & cos\theta_3 & 0 & y_{2,n} \\ 0 & 0 & 1 & 0 \\ 0 & 0 & 0 & 1 \end{bmatrix}. \quad (10) $$

Where θ_3 is the angle between the tangent of the second segment (active segment) at its tip and the X_0-axis. Furthermore, by using expressions (7), (8), (9) and (10) the full three-segment structure can be given as:

$$SF_3 = \begin{bmatrix} {}^1M_0\, C_P^1 & {}^1M_0{}^2M_1\, C_A^2 & {}^3M_2{}^2M_1{}^1M_0\, C_P^1 \end{bmatrix} = \begin{bmatrix} 0 & l_1 & l_1 & x_{2,1}+l_1 & .. & x_{2,n}+l_1 & x_{2,n}+l_1 & x_{2,n}+l_1+l_3\, cos\theta_3 \\ 0 & 0 & 0 & y_{2,1} & .. & y_{2,n} & y_{2,n} & y_{2,n}+l_3\, sin\theta_3 \\ 0 & 0 & 0 & 0 & .. & 0 & 0 & 0 \\ 1 & 1 & 1 & 1 & .. & 1 & 1 & 1 \end{bmatrix} \quad (11)$$

The expression (11) is $[4 \times n+5]$ matrix, which is the concatenation of first segment matrix $[4 \times 2]$, second segment matrix $[4 \times n+1]$ and third segment matrix $[4 \times 2]$. It allows the modeling of the folding behavior of the three-segment structure. The angle θ_3, also known as the folding angle of the structure, depends on the curvature of the active segment (second segment), which is induced by the applied voltage.

2.2 Origami cube model

The model of the self-folding origami cube is a 3D one and it uses one applied voltage to control all active segments. The model contains 14 segments: 9 passive segments (1, 2, 4, 6, 8, 9, 11, 12 and 14) and 5 active segments (3, 5, 7, 10 and 13), as shown in Fig. 2. Contrarily to the 2D model discussed above, some joints connect more than two segments. In this case, one joint connects four segments (1, 2, 9 and 12). Furthermore, segments from 1 to 8 are all in the plan (X,Y), which means that their orientation angle ϕ is equal to 0. As for segments 9 to 14 they are all in the plan (Y,Z). Nonetheless, the orientation angle ϕ for the segments 9 to 11 is $\frac{\pi}{2}$ and for segments 12 to 14 is $-\frac{\pi}{2}$, as shown in Tab. 1. However, for the sake of brevity, the model will not be developed here.

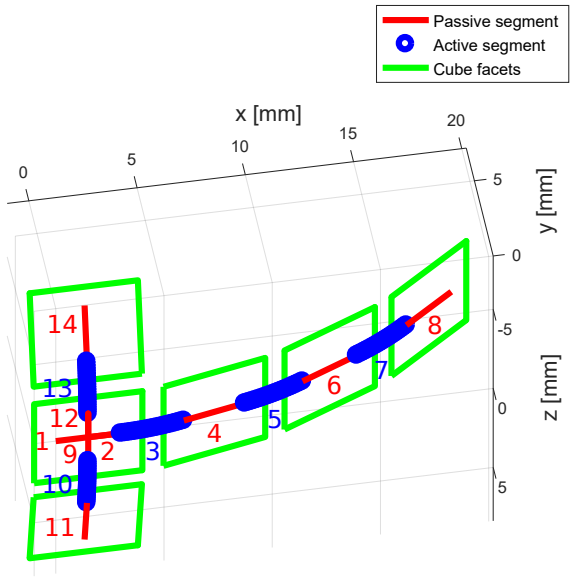

FIGURE 2. kinematic model of the self-folding origami cube for an applied voltage of 0.1 V.

TABLE 1. List of variable for the origami cube model.

Segment	Type	Length (mm)	width (mm)	Orientation angle ϕ (rad)
1	passive	3	5	0
2	passive	3	5	0
3	active	2	1	0
4	passive	3	5	0
5	active	2	1	0
6	passive	3	5	0
7	active	2	1	0
8	passive	3	5	0
9	passive	3	5	$\frac{\pi}{2}$
10	active	2	1	$\frac{\pi}{2}$
11	passive	3	5	$\frac{\pi}{2}$
12	passive	3	5	$-\frac{\pi}{2}$
13	active	2	1	$-\frac{\pi}{2}$
14	passive	3	5	$-\frac{\pi}{2}$

3 Experimental validation

The aim of this section is to discuss the fabrication process of the tri-layered CP actuators, utilized in the proposed self-folding approach. Then, the experimental setup is presented. Next, the model of self-folding three-segment structure (passive/active/passive) is experimentally validated. Finally a proof of concept of a more complex origami-based structure (origami cube) is presented.

3.1 Materials and experimental setup

An electropolymerization three-electrode system process is utilized for the fabrication of the tri-layered CP actuators. The three-electrode system is linked to a potentiostat OrigaFlex-OGF500 from OrigaLys ElectroChem SAS and it is controlled by OrigaMaster5[1] software. More details about the electropoly-

[1] http://www.origalys.com/origasoft-logiciel-pc-origamaster-c2x19668303

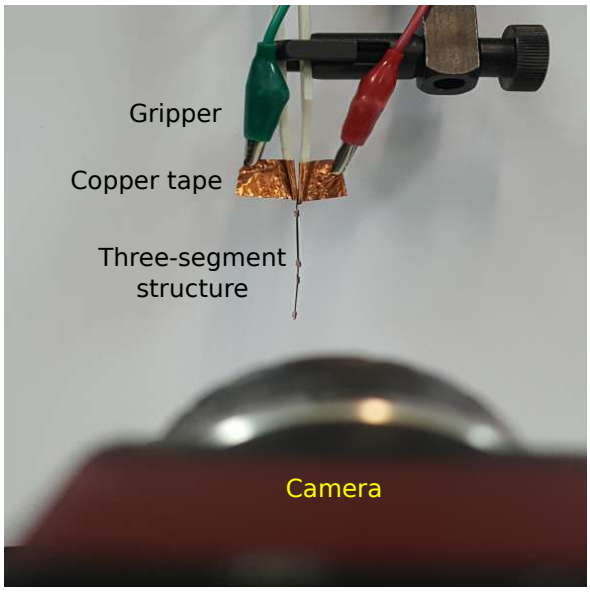

FIGURE 3. Experimental setup for the characterization of the CP actuator-based self-folding structures.

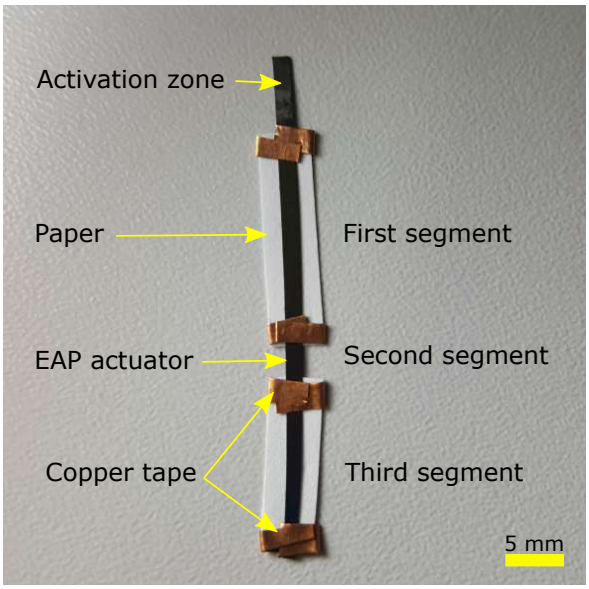

FIGURE 4. Top view of the three-segment self-folding straight structure.

merization process are provided in the work of Cot et al [20], which is a similar process to the one used in this work.
A test bench was mounted in order to characterize the three-segment structure. It was based on MATLAB Simulink software using Visual Servoing Platform (ViSP) and a dedicated blockset cvlink[2]. The self-folding structures were hugged from a gripper covered by conductive copper tape from each side, to allow electric simulation of the structure, as shown in Fig. 3. The gripper is also used to constrain the first segment, so it will not move during the experimental testing. The applied voltage is provided via a National Instruments multifunction data acquisition module (USB-6211), which can generate voltage between $\pm$ 10 V with a resolution of 3.5 mV. A camera (IEE 1394 Guppy Firewire) is placed in front of three-segment structure in manner that allows the visualization of the structure thickness.

3.2 Three-segment structure

The main objective of this subsection is to experimentally validate the model for the three-segment self-folding structure. First, a 41 mm long and 3 mm wide strip of the tri-layered CP actuator was cut using a sharp scalpel. Then, two strips of paper (15×5 mm^2 and 20×5 mm^2) were glued to each end of the actuator: the two paper strips were put against each end of the CP actuator, then using small pieces of tape they were glued to the actuator (as shown in Fig. 5). The paper strips were utilized in order to rigidify certain regions of the actuator where bending is not needed (both its ends), and to allow the design of the self-folding three-segment structure: tow passive (rigid segments) linked by an active segment (bendable). The dimensions of the segments are 15×5 mm^2, 6×3 mm^2 and 20×5 mm^2, from the first to the third segment, respectively. The three-segment structure was mounted into the experimental setup and series of experimental tests were conducted. For different applied voltages (from 0.2 to 0.7 V), the behavior of the studied structure was observed and compared to the model discussed above. The results are shown in Fig. 5. An applied voltage of 0.2 V induces a folding angle of about 38°. Then, for each additional 0.1 V to the applied voltage, the folding angles gains approximately 10°, until it reaches almost 90° for a voltage of 0.7 V as shown in Tab. 2. One can notice that even though the paper strips help maintain the passive segments rigid, their weight (less than 10 mg) has a negligible effect on the folding motion. However, if their weight exceeds the 100 mg, it will have a very negative effect on the folding motion as well as the maximum folding angle.

TABLE 2. The folding angles of the three-segment structure.

Applied voltage (V)	0.2	0.3	0.4	0.5	0.6	0.7
Folding angle (°)	37.8	51.4	61.7	71.7	81.1	89.6

The proposed model is able to simulate the behavior of the three-segment structure (the folding) with RMS error of 1.3° as shown in Tab. 3, which less than 1.5 % of the maximum folding

[2]https://sourcesup.renater.fr/cvlink/

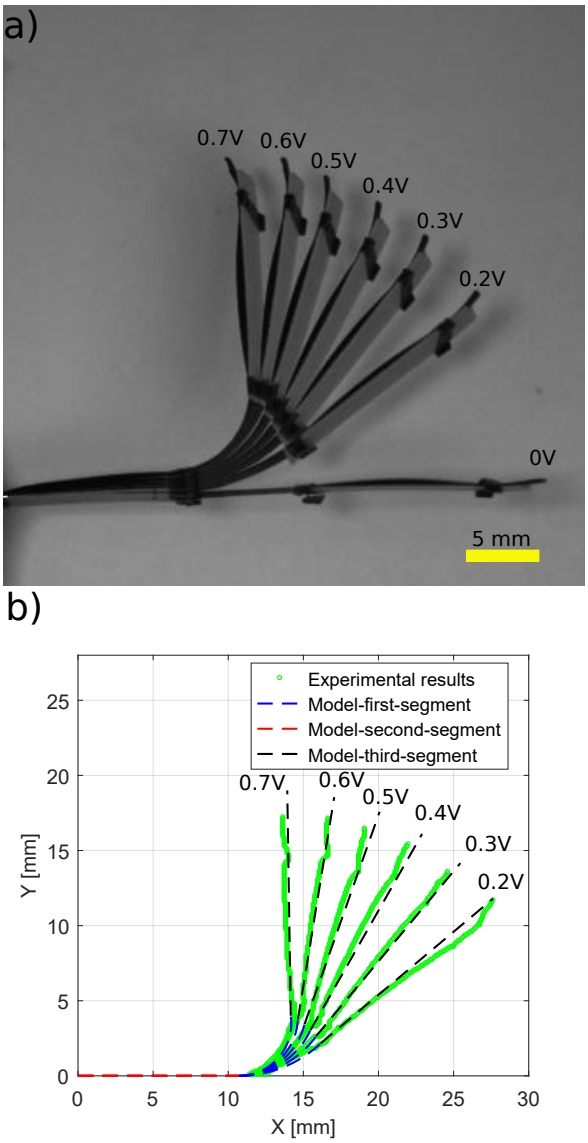

FIGURE 5. Three-segment self-folding structure: a) responses for an applied voltage varying from 0.2 to 0.7 V obtained through superimposition of images, and b) comparison of the experimental results to the model.

angle. It can be concluded that the model works well and can be utilized to simulate more complex self-folding structures and designs.

3.3 Proof of concept

As proof of concept for more complex self-folding structures based on CP actuators, the folding of an origami cube was tested. The design of origami cube contains three types of components: (i) a T-shaped CP actuator, which was cut using a sharp scalpel, (ii) a 3×3 mm^2 squares of double-sided copper tape and (iii) 5×5 mm^2 squares of paper (see Fig. 6). Five copper tape squares were used in the fabrication of the 2D design of the origami cube. They were glued to the T-shaped CP actuator to act as 3 mm passive segments. The reason behind using copper taper instead of regular tape is, to avoid the bending of the passive segments by the CP actuator. Each copper square (passive segment) was at a distance of 2 mm from the next ones. In other words, the length of the active segments is 2 mm, and they have a width of 1 mm. Finally, the 5×5 mm^2 paper squares were glued on top of the copper tape squares in order to compensate for the some-what long active segment and to ensure a closed cube-shaped structure. Shorter active segment can be used, however in this case higher voltages (around 2 V) are needed to achieve the folding. Nonetheless, the high voltage can gradually damage the CP actuator and drastically lower its performance. The effect of the damage can be easily observed after few cycles of activation. However, this not the case for an applied voltage of 0.7 V or less. The CP actuator suffers zero damage, no matter how many activation cycles are performed.

An applied voltage of 0.7 V was used to activate the self-folding mechanism of the origami cube. The results are shown in Fig. 7.

TABLE 3. Error of the model for the three-segment structure.

RMS (°)	STD (°)	MAX (°)	MIN (°)
1.3	0.5	2.2	0.4

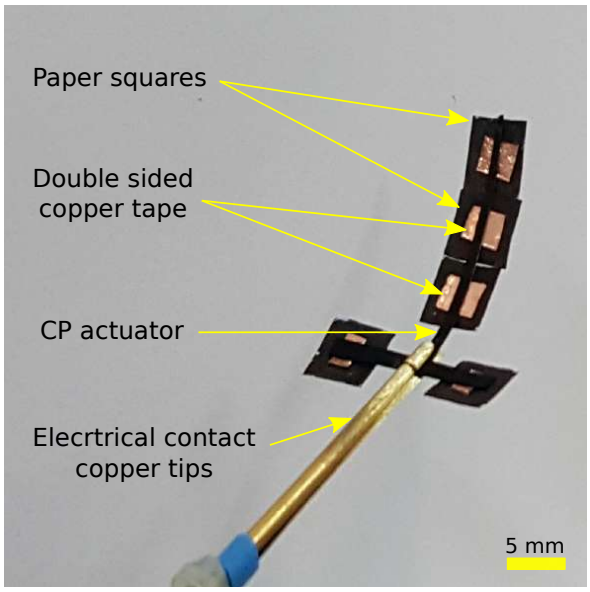

FIGURE 6. Top view of the 2D design of the self-folding origami cube.

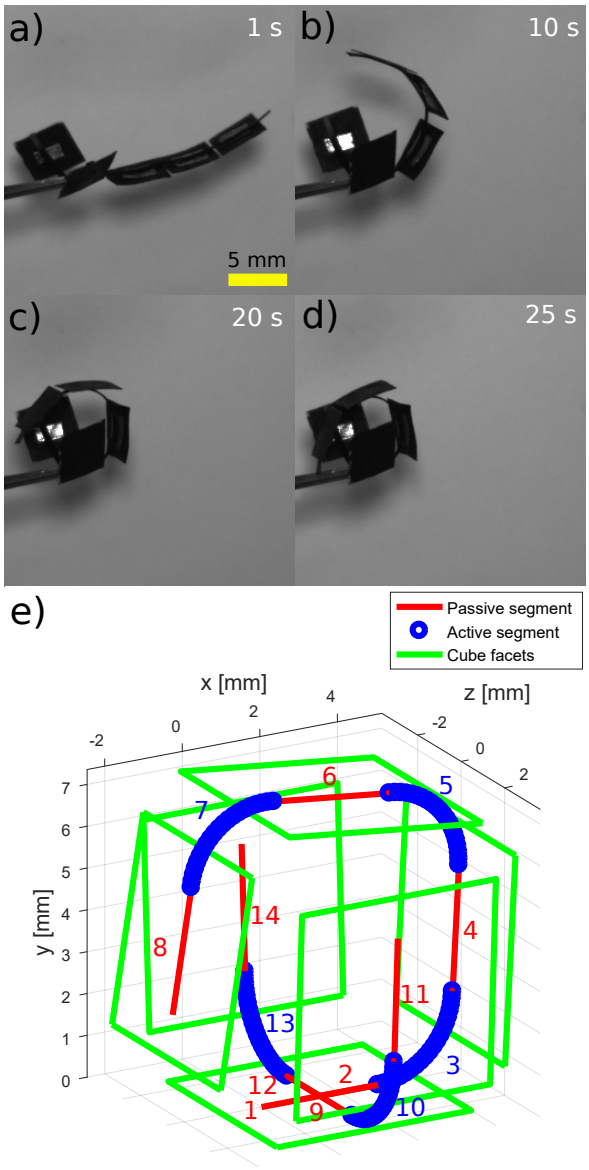

FIGURE 7. Folding of the origami cube for an applied voltage of 0.7 V: time laps of the experimental folding a) at 1 s b) at 10 s c) at 20 s d) at 25 s and e) self-folding simulation model.

The model was able to estimate the behavior of the self-folding origami cube. Nonetheless, even by exploiting the model, it will not be enough to achieve more precise folding, because the manual cutting really limits this approach, in terms of the complexity and the accuracy of the cut shapes. For instance, it will helpful to have the same width along the whole cut shape, in order to have a uniform behavior (i.e. the same folding angle from all active segments) for the self-folding structure. Furthermore, to overcome such limitations, laser machining has to be used during the fabrication process. Laser testing is currently in progress, in order to find a suitable adjustment of machining the CP actuators without affecting their performance.

4 Conclusion

In this paper an approach for self-folding structures based on CP actuators is discussed. A kinematic model for simulating the behavior of such systems is proposed. The model contains two types of segments: passive segments rigidified using paper or copper tape, and active segments made of CP actuators. Furthermore, since the maximum used voltage is 0.7 V, one can conclude that using CP actuators allows for energy efficient self-folding approach, without compromising the large and reversible folding behavior. An origami cube was used as a proof of concept for more complex self-folding systems. The next step is to design even more complex origami bases, such as the waterbomb base. The designed structures will be developed for biomedical applications in confined spaces such as navigating or delivering drug in the human body.

ACKNOWLEDGMENT

This work has been supported by the Labex ACTION project (contract ANR-11LABX-0001-01), CoErCIVe Bourgogne Franche-Comté regional project, and μRoCS project (contract ANR-17-CE19-0005-04).

REFERENCES

[1] Zirbel, Shannon A., et al."Accommodating thickness in origami-based deployable arrays." *Journal of Mechanical Design* 135.11 (2013): 111005.

[2] Kuribayashi, Kaori, et al. "Self-deployable origami stent grafts as a biomedical application of Ni-rich TiNi shape memory alloy foil." *Materials Science and Engineering:* A 419.1-2 (2006): 131-137.

[3] Bassik, Noy, et al. "Enzymatically triggered actuation of miniaturized tools." *Journal of the American Chemical Society* 132.46 (2010): 16314-16317.

[4] Edmondson, Bryce J., et al. "Oriceps: Origami-inspired forceps." *Conference on smart materials, adaptive structures and intelligent systems.* American Society of Mechanical Engineers, 2013.

[5] Miyashita, Shuhei, et al. "Ingestible, controllable, and degradable origami robot for patching stomach wounds." *Robotics and Automation (ICRA),* International Conference on. IEEE, 2016.

[6] Benouhiba, Amine, et al. "An Origami-Based Tunable Helmholtz Resonator for Noise Control: Introduction of the Concept and Preliminary Results." *Conference on Smart*

Materials, Adaptive Structures and Intelligent Systems. American Society of Mechanical Engineers, 2017.

[7] Hawkes, Elliot, et al. "Programmable matter by folding." *Proceedings of the National Academy of Sciences* 107.28 (2010): 12441-12445.

[8] Tolley, Michael T., et al. "Self-folding origami: shape memory composites activated by uniform heating." *Smart Materials and Structures* 23.9 (2014): 094006.

[9] Ahmed, Saad, et al. "Multi-field responsive origami structures: Preliminary modeling and experiments." *International Design Engineering Technical Conferences and Computers and Information in Engineering Conference.* American Society of Mechanical Engineers, 2013.

[10] Paik, Jamie K., and Robert J. Wood. "A bidirectional shape memory alloy folding actuator." *Smart Materials and Structures* 21.6 (2012): 065013.

[11] Peraza-Hernandez, Edwin, et al. "Design and optimization of a shape memory alloy-based self-folding sheet." *Journal of Mechanical Design* 135.11 (2013): 111007.

[12] Kim, Sa-Reum, et al. "Fast, compact, and lightweight shape-shifting system composed of distributed self-folding origami modules." *Robotics and Automation (ICRA),* International Conference on. IEEE, 2016.

[13] Miyashita, Shuhei, Cagdas D. Onal, and Daniela Rus. "Self-pop-up cylindrical structure by global heating."*Intelligent Robots and Systems (IROS),* International Conference on. IEEE, 2013.

[14] Na, JunHee, et al. "Programming reversibly selffolding origami with micropatterned photocrosslinkable polymer trilayers." *Advanced Materials* 27.1 (2015): 79-85.

[15] Miyashita, Shuhei, et al. "An untethered miniature origami robot that self-folds, walks, swims, and degrades." *Robotics and Automation (ICRA)*, International Conference on. IEEE, 2015.

[16] Silverberg, Jesse L., et al. "Origami structures with a critical transition to bistability arising from hidden degrees of freedom." *Nature materials* 14.4 (2015): 389.

[17] Liu, Ying, et al. "Self-folding of polymer sheets using local light absorption." *Soft Matter* 8.6 (2012): 1764-1769.

[18] Liu, Ying, et al. "Three-dimensional folding of pre-strained polymer sheets via absorption of laser light." *Journal of Applied Physics* 115.20 (2014): 204911.

[19] Liu, Ying, et al. "Sequential self-folding of polymer sheets." *Science Advances* 3.3 (2017): e1602417.

[20] Cot, Amélie, et al. "Synthesis, encapsulation, and performance analysis of large deformation tri-layer polypyrrole actuator." *Advanced Intelligent Mechatronics (AIM)*, International Conference on. IEEE, 2016.

[21] Kim, J. I., "Compact multi-physics models for large-displacement multilayer cantilevers in RF MEMS circuits, antennas and sensors". *Doctoral dissertation, Purdue University*, 2008.